# Spectroscopic Studies of the Effects of Selenate and Selenite on Cobalt Sorption to γ-Al 2 O 3

**ARTICLE** *in* ENVIRONMENTAL SCIENCE AND TECHNOLOGY · MARCH 2002

Impact Factor: 5.33 · DOI: 10.1021/es001774i



**3 AUTHORS**, INCLUDING:

Lynn Katz
University of Texas at Austin
**68** PUBLICATIONS **878** CITATIONS

*Environ. Sci. Technol.* **2002**, *36,* 1219−1225

# Spectroscopic Studies of the Effects of Selenate and Selenite on Cobalt Sorption to $\gamma$-$Al_2O_3$

ERIC J. BOYLE-WIGHT

*Department of Civil and Environmental Engineering, University of Maine, Orono, Maine 04469*

LYNN E. KATZ*

*Department of Civil and Environmental Engineering, ECJ 8.6, University of Texas, Austin, Texas 78712*

KIM F. HAYES

*Department of Civil and Environmental Engineering, The University of Michigan, Ann Arbor, Michigan 48109*

The fate and transport of toxic metal ions and radionuclides in the environment is often controlled by sorption reactions. The extent of sorption of divalent metal cations is controlled by a number of factors including the presence of cosorbing or complexing ligands. To study the impact of anion cosorption on metal cation sorption behavior, Co(II) sorption to $\gamma$-$Al_2O_3$ in the presence of selenium oxyanions was investigated. To aid in the interpretation of macroscopic sorption results, X-ray absorption spectroscopy (XAS) experiments were conducted on single and bisorbate samples where the Co(II) surface coverage of the bisorbate sample was greater than or equal to the single sorbate sample. XAS data for single sorbate Co(II) samples were consistent with reported spectra of Co(II)-Al(III) layered double hydroxides (LDHs), indicating coprecipitates are forming in these samples. Comparison of data from single and bisorbate samples showed a decrease in the number of nearest neighbor cobalt atoms in the presence of Se(IV), irrespective of the order of Se(IV) addition and no change in Co coordination in the presence of Se(VI). The extent of the decrease in cobalt second shell features between single and bisorbate samples with equal Co(II) coverage increased with an increase in the Se:Co surface coverage ratio. This trend suggests that the effect of Se(IV) on Co(II) sorption is a function of the Se(IV) surface coverage. At low ratio values, Co(II)-Al(III) LDH precipitates dominate. Increasing the Se:Co surface coverage ratio results in a progressive conversion of coprecipitate to an unknown, disordered Co(II)/Se(IV) phase. Based on macroscopic data, this new phase could be an LDH with Se(IV) in the interlayer, an alternative precipitate such as a mixed metal Se(IV) hydrate, or a ternary complex.

## Introduction

Although toxic metal ions are naturally present at low levels in the environment, elevated levels are often observed in surface and subsurface soils as a result of human activities. These inorganic contaminants in the environment are affected by a number of reaction processes. Metal speciation, mobility, and bioavailability are often controlled by partitioning (or sorption) processes at the solid−water interface in soils and sediments. Distinguishing between different types of sorption complexes and understanding the factors controlling the particular type of sorption complex formed is essential for developing predictive fate and transport models. Research conducted over the past several decades has helped to identify the types of sorption complexes that form in single-sorbate systems (*1*), and this information has been used to guide the development of predictive sorption models (*2*−*4*). However, there is a need to extend this work to more realistic systems containing multiple sorbates and sorbents. For example, few studies have addressed the impact of strongly sorbing oxyanions on metal cation sorption even though these contaminants often appear in the same waste streams.

In a companion paper (*5*), results from macroscopic uptake experiments were used to identify the effect of strongly sorbing Se(IV) and weakly sorbing Se(VI) oxyanions on Co(II) sorption to $\gamma$-$Al_2O_3$. Batch equilibrium sorption experiments showed that Co(II) sorption to $\gamma$-$Al_2O_3$ was altered by the presence of Se(IV) but not Se(VI). The presence of Se(IV) caused either no effect or an increase in Co(II) sorption at Co(II) surface coverage < 0.1 $\mu$mol/m$^2$ as a function of anion concentration. At Co(II) surface coverage > 0.5 $\mu$mol/m$^2$, Se(IV) decreased Co(II) sorption when Se(IV) was added at the same time as Co(II). However, Co(II) was retained when Co(II) was sorbed in the absence of Se(IV) and then treated with Se(IV) and nitric acid to lower the pH. Based on these data we hypothesize that a change in the structure of the sorbed Co(II) is occurring under high surface loading conditions.

While macroscopic data provides invaluable information about trends in metal ion uptake as a function of various solution conditions, sorption mechanisms cannot be elucidated from this scale of investigation. Molecular scale data are required to differentiate between adsorption, precipitation, or coprecipitation mechanisms. X-ray absorption spectroscopy (XAS) was chosen as the primary molecular scale technique to be used in this work as it can be used to gain information in situ about oxidation state (X-ray absorption near edge structure (XANES)) and local structure (extended X-ray absorption fine structure (EXAFS)). XAS provides information about the local structural environment around a specific target atom such as coordination state, neighboring atoms, and structural distances to approximately 6 Å. Unfortunately, a collection of usable spectroscopic data is difficult below surface coverages of 0.1 $\mu$mol/m$^2$ in these systems, limiting XAS studies to the higher coverage samples. In this study, we extend our recently reported investigation of cobalt/selenium bisorbate systems (*5*) to examine the structural changes occurring in multisorbate systems containing Co(II) at surface coverages greater than 0.5 $\mu$mol/m$^2$ and Se(IV) or Se(VI) at surface coverages greater than 1.0 $\mu$mol/m$^2$.

**Background.** Cobalt(II) sorption has been studied extensively on both oxide (*1*, *6*−*11*) and clay (*12*−*15*) surfaces. At low surface loadings (less than 0.25 $\mu$mol/m$^2$), Co(II) sorbs to alumina as a mononuclear complex (*10*, *16*). Studies on $\gamma$-$Al_2O_3$ found that increasing the surface loading to greater than 0.5 $\mu$mol/m$^2$ resulted in polymeric Co(II) structures that increase in number or size with increasing coverage (*10*). The nature of the cluster structure is similar to a hydroxide precipitate except that distances are typically shorter than $Co(OH)_2$ with a Co−O distance of 3.08 Å as compared to 3.10

* Corresponding author phone: (512)471-4244; fax: (512)471-5870; e-mail: lynnkatz@mail.utexas.edu.

10.1021/es001774i CCC: $22.00 
Published on Web 02/16/2002

**TABLE 1. Surface Coverage Data and Fit Parameters for Cobalt EXAFS**

| | | surface coverage data | | | first shell Co−O | | | second shell Co−Co | | |
|---|---|---|---|---|---|---|---|---|---|---|
| sample | pH | $\Gamma_{Co}$ | $\Gamma_{SeO3}$ | $\Gamma_{SeO4}$ | *N* | *R* | $\sigma^2$ | *N* | *R* | $\sigma^2$ |
| MC1 | | $Co(OH)_2$ 40 mg/1 g BN | | | 6.00[F] | 2.10[F] | 0.004 | 6.00[F] | 3.17[F] | 0.003 |
| PPT | 7.59 | Co:Al = 2.02 | | | 6.12 | 2.08 | 0.006 | 3.89 | 3.10 | 0.006 |
| SS1 | 7.40 | 2.1 | | | 6.08 | 2.08 | 0.005 | 2.84 | 3.08 | 0.003 |
| BS1 | 7.67 | 2.1 | 1.7 | | 6.12 | 2.08 | 0.005 | 2.55 | 3.09 | 0.005 |
| BS2 | 7.32 | 1.0 | | 3.9 | 6.26 | 2.09 | 0.005 | 2.94 | 3.10 | 0.006 |
| SS2 | 7.26 | 0.7 | | | 5.90 | 2.08 | 0.006 | 1.58 | 3.09 | 0.004 |
| BS3 | 7.51 | 0.8 | 1.3 | | 5.67 | 2.07 | 0.006 | 0.92 | 3.11 | 0.006 |
| BS4 | 7.50 | 0.8 | 1.6 | | 5.43 | 2.07 | 0.006 | | | |
| SOL1 | 4.50 | 0.01 M $Co(NO_3)_2$ | | | 5.86 | 2.08 | 0.004 | | | |
| SS4 | 7.59 | 1.05 | | | 6.01 | 2.07 | 0.005 | 2.56 | 3.08 | 0.004 |
| BS5 | 7.46 | 1.37 | 1.50 | | 6.09 | 2.08 | 0.008 | 0.96 | 3.12 | 0.007 |

[F] Indicates that these values were fixed based on known crystallographic data.

Å and Co−Co distance of 3.09 Å compared to 3.17 Å (*9*, *10*). In the majority of samples examined in these studies, metal ion concentrations were below metal hydroxide solubilities. Reexamining data of Chisholm-Brause (*9*) and O'Day (*17*), Charlet and Manceau (*18*) proposed that neoformation of clay structures similar to kerolite and Co-sepiolite can explain polynuclear Co(II) on silicate minerals such as $SiO_2$ and kaolinite. The local structure around cobalt in these clays contains the same shortened distances relative to $Co(OH)_2$ observed in the sorption samples. Similar studies have shown that hydrotalcite-like clays can form during metal ion sorption to many mineral surfaces including Ni sorption to pyrophyllite (*19*, *20*) and Co sorption to $\gamma$-$Al_2O_3$ (*11*) and kaolinite (*21*).

The limiting factor for coprecipitation is considered to be Al(III) dissolution from the surface. In one case, alumina was isolated from the metal solution by a membrane (*22*). Coprecipitates with a hydrotalcite-like structure were found to form inside and outside the dialysis membrane, indicating that coprecipitation is not necessarily occurring at the surface. Thompson (*23*) showed that the rates of hydrotalcite precipitation are a function of the Al source phase where the presence of more readily dissolving phases such as aluminum hydroxide increases coprecipitation. An important attribute of hydrotalcite precipitation is that solubilities are below those of metal hydroxides.

These hydrotalcite phases consist of brucite-like layers of edge-sharing metal octahedra interlayered by charge-compensating anions. The interlayer anions are required to compensate the excess positive charge imparted by Al(III) substitution into the octahedral layer. In most previous studies examining the formation of these phases during sorption of divalent metal ions, the only interlayer anions present have been nitrate (added as a background electrolyte), silicates (from dissolution of clay minerals), and carbonates (from absorption from the atmosphere). In systems containing other anions, especially strongly sorbing anions, the formation of these hydrotalcite phases may be altered.

In this study we examine the effect of Se(IV), added as a strongly sorbing oxyanion, and Se(VI), added as a weakly sorbing oxyanion, on Co(II) sorption under conditions where coprecipitation is the predominant sorption mechanism in corresponding single sorbate Co(II) systems. The objective of this study was to elucidate the changes occurring in the structure of sorbed Co(II) in the presence of selenium oxyanions that are responsible for the significant alteration in Co(II) sorption.

## Experimental Methods

**Sorption Samples.** Batch equilibrium studies were conducted using 0.5 $\mu$m $\gamma$-$Al_2O_3$ (Buehler Alumina), $Co(NO_3)_2$, $Na_2SeO_3$, $Na_2SeO_4$, and $NaNO_3$ (Johnson Matthey Co.). Metal stock solutions were prepared using double deionized boiled water (Nanopure) in 0.01 M $HNO_3$ and stored in a nitrogen atmosphere. Samples were prepared in a nitrogen glovebox by adding the required quantities of Nanopure water, $\gamma$-$Al_2O_3$ slurry, $NaNO_3$, and metal stock solutions to centrifuge tubes or bottles. The pH was adjusted incrementally with NaOH starting below the point where sorption begins and using small aliquots to prevent $Co(OH)_2$ saturation. Base additions of carbonate free 0.1 M NaOH (Dilut-IT, J. T. Baker) were made a minimum of 2 h apart and after the final addition equilibrated for at least 12 h. Samples were centrifuged at 12 000 rpm for 40 min after pH measurement in order to remove all particles greater than 0.1 $\mu$m. Solute analysis on the supernatant was conducted using flame atomic absorption. Samples for XAS were prepared by aspirating the supernatant from centrifuged samples and mounting the wet paste in aluminum cryostat samples cells while in the nitrogen glovebox. Samples were then immediately frozen in liquid nitrogen.

During preparation of EXAFS samples, care must be taken to isolate the pH effect on coprecipitate formation from a possible Se(IV) competitive effect because surface coverage increases with increasing pH in the region of the sorption edge. To this end, EXAFS samples were prepared on an equal Co(II) surface coverage basis, requiring the single and bisorbate samples to be prepared at a different pH. Three sets of single and bisorbate samples with Co(II) surface coverages ($\Gamma$) ranging from 0.8 to 2.1 $\mu$mol/m$^2$ were examined (Table 1).

**Precipitate Sample.** A cobalt−aluminum hydrotalcite-like precipitate was prepared following methods similar to Taylor (*24*) where parent solutions were maintained below the cobalt hydroxide solubility. Solutions of 1.0 M $Co(NO_3)_2$ and 0.5 mM $Al(NO_3)_2$ with an ionic strength equal to 0.01 M $NaNO_3$ were adjusted to a pH of 7.5. The solutions were combined, and the sample was rapidly mixed at a pH of 7.5. The pH was maintained for 6 h through NaOH (Dilut-IT, J. T. Baker) addition using a Radiometer model PHM 290 pH Stat. The entire operation was conducted under a nitrogen atmosphere to avoid carbonate intrusion. The resulting precipitate was centrifuged, decanted, and freeze-dried. XRD data showed the sample to be largely X-ray amorphous with broad peaks at approximately 22, 35, and 60 degrees, consistent with Co(II)-Al(III)-$CO_3^{2-}$ hydrotalcite-like precipitates reported by Thompson et al. (*21*).

**XAS Data Analysis.** EXAFS spectra were collected at the Stanford Synchrotron Radiation Laboratory (SSRL) on wiggler beam lines 7-3 and 4-2. Data for solution samples SOL1 and SOL2 and one sorption sample, SS5, were collected at room temperature. All other data were collected at cryogenic temperatures (20 K) using a liquid He cryostat sample holder to minimize static disorder. With the exception of improved

signal-to-noise at low temperatures, no difference was found between room and cryogenic temperatures. Beam current ranged from 40 to 95 mA at 3 GeV with a wiggler magnetic field of 18 kG. Energy selection was achieved using a Si(220) crystal monochromator with incoming beam flux detuned 30−50% to reject high-order harmonic reflections. Beam energy was calibrated to the *K*-edge of a metallic Co foil at 7709.5 eV or elemental Se foil at 12 658 eV. Fluorescence spectra for low-temperature samples were collected using a 13 element Ge detector with a Be window at a 45° angle to the sample. Fluorescence spectra for the solution samples were collected using a Stern-Heald-type detector (*25*) with soller slits, $N_2$ gas, and an Al filter. Solid samples were mounted in 6 mm sample holders and covered with Teflon tape. Solid standards were diluted in boron nitride (BN) to the same mass concentration range as the samples (approximately 40 mg/g BN depending on the standard). Self-absorption effects were limited by working with low mass concentration samples. Comparisons between fluorescence and transmission data for the most concentrated samples showed no significant self-absorption effects. Sorption samples typically required 6−12 scans depending on concentration. Model compounds of known structure typically required 2−4 scans.

Data analysis was accomplished using a suite of programs developed at SSRL called EXAFSPAK (*26*). Background below the absorption edge was subtracted using a Gaussian fit through the preedge region. Background above the absorption edge was subtracted using a fourth order, three segmented spline fit through the EXAFS region using a Victoreen polynomial and tabulated McMaster coefficients (*27*−*29*). The energy at which wavevector $k$ was set to zero ($E_0$) was 7725 eV for Co and 12 675 eV for Se. Damping of the spectra was compensated by weighting with a factor of $k^3$. A $k$-space EXAFS range was selected using points at which Chi was zero, typically 3.0−13.0. The $k$-window range was then Fourier transformed to distance space, producing radial structure functions (RSF). Individual peaks and groups of peaks were isolated with a window in R-space and back-transformed. Generally, an experimental model compound was first analyzed to determine spline conditions and R-windows, which were altered minimally for the sample analysis.

Fitting to extract structural information was accomplished by nonlinear least squares techniques with four adjustable parameters per component: $N$, $R$, $\sigma^2$, and $\Delta E_0$ where $N$ is the coordination number, $R$ is the distance, $\sigma^2$ is the Debye−Waller factor, and $\Delta E_0$ is the difference between the reference functions and unknown spectra. The $\Delta E_0$ variable was floated in the first shell only and fixed in subsequent shells. Theoretical phase-shift and amplitude functions were generated using FEFF 7.0 (*30*) for $Co(OH)_2$, $Al_2(SeO_3)\cdot 6H_2O$ or $Na_2SeO_3$, and $Na_2SeO_4$. In some cases, structural data was not available for generating true FEFF models. One such case was the Co−Al distance expected to be present for innersphere Co complexes and hydrotalcite-like coprecipitates. A Co−Al scattering path was generated by substituting Al for Co in the $Co(OH)_2$ structure without changing the distance. FEFF was run using a cluster radius of no longer than 7 Å, Debye−Waller values set to zero (for theoretical calculations) and $S_0$, an amplitude scaling factor, set to 0.9. Individual path $k$-Chi data were imported in EXAFSPAK, and a single phase and amplitude file was compiled that included all potentially significant paths.

Data analysis consisted of first fitting experimental model compound data with theoretical phase and amplitude functions, verifying the scaling factor, $S_0$. Fits to unknown sample spectra were accomplished in a series of steps starting with individual RSF peak windows followed by fits to R-windows containing both first and second shells. During the final step, all parameter data were combined to fit the original $k^3$ EXAFS spectra.

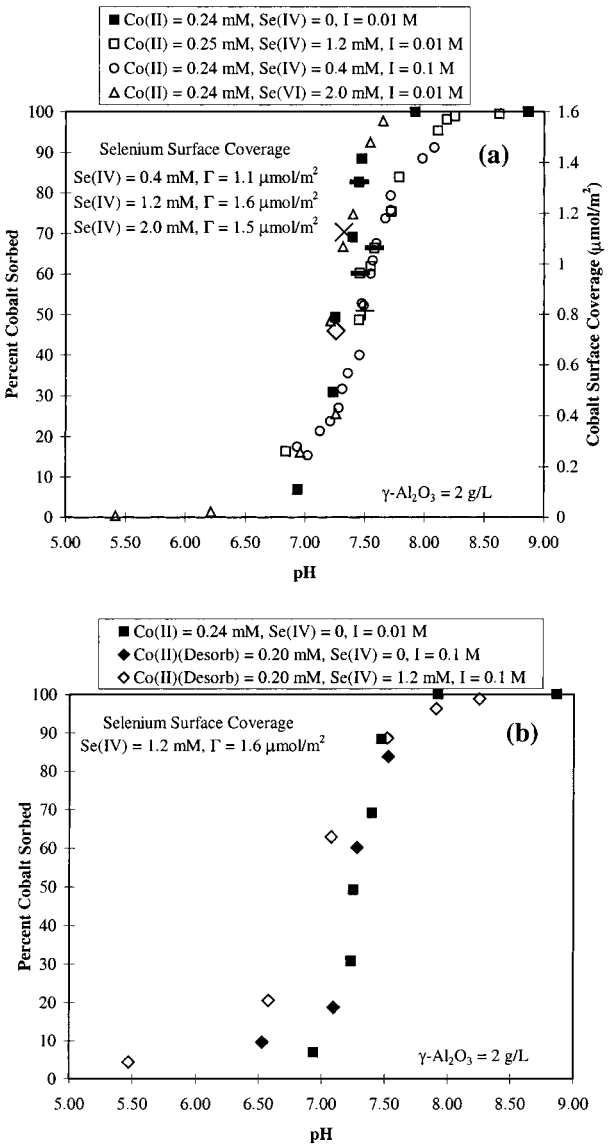


**FIGURE 1. (a) Co(II) sorption to $\gamma$-$Al_2O_3$. XAS samples are represented by the following: sample 4 = X, sample 5 = ◇, sample 7 = +. Samples crossed with lines are sorption samples that have equilibrated for 2 weeks (see Table 3). (b) Co(II) desorption from $\gamma$-$Al_2O_3$ with and without the presence of Se(IV) (Co single-sorbate sorption data are shown for comparison).**

## Results

**Macroscopic Sorption Results.** Preparation of sorption samples typically began at a low pH with both Co(II) and Se present, resulting in Se sorbing prior to Co(II). Figure 1a shows that the presence of Se(IV) decreased Co(II) sorption of the pH range 7.25−8.25, while Se(VI) had no effect on the location of the pH sorption edges compared to single-sorbate data. Equilibrating the bisorbate samples for 2 weeks compared to 2 days resulted in an equivalent reduction in Co(II) sorption in the presence of Se(IV) (Figure 1a, symbols crossed with lines), indicating that the decrease in sorption is most likely not a rate effect. In a second set of experiments, 95% of the initial Co(II) concentration was sorbed (at surface coverages greater than or equal to1 $\mu$mol/m$^2$) prior to the introduction of Se(IV) and then desorbed by lowering the pH in the absence and presence of Se(IV). These desorption results show enhanced retention of Co(II) in the presence of

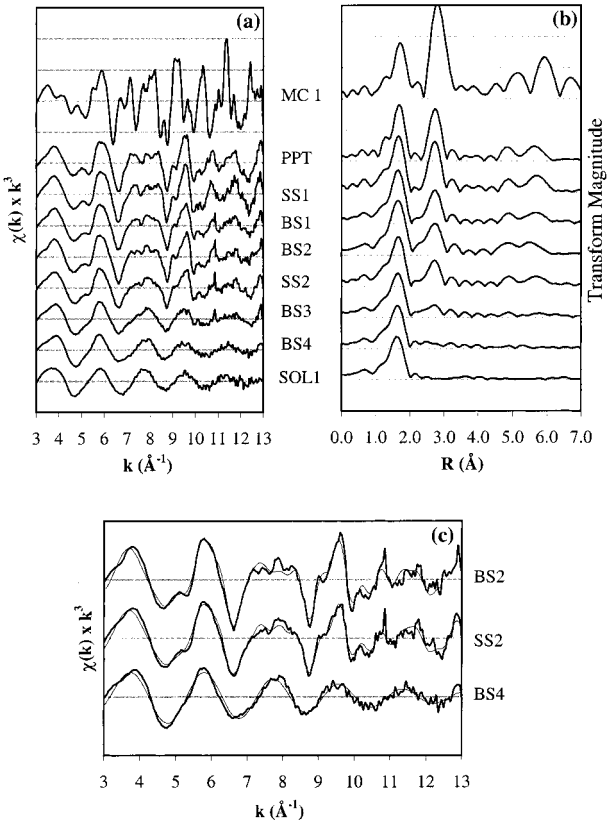


**FIGURE 2. Cobalt EXAFS results. (a) Background subtracted, *k*-weighted cobalt EXAFS spectra. (b) Radial structure functions of Fourier transformed EXAFS. (c) Fit examples representative of the fit quality. Heavy lines are the data and fine lines are the fits using parameters in Table 2. See Table 1 for sample identification.**

Se(IV) relative to single sorbate Co(II) desorption samples that coincide with the single-sorbate sorption data collected under approximately the same conditions (Figure 1b). The enhancement in sorption is most notable at lower surface coverages. At higher surface coverages, the bisorbate and single-sorbate desorption data coincide. The lack of hysteresis in the Co(II) single sorbate data suggests that Co(II)-Al(III) coprecipitates are not responsible for the retention, and, thus, Se(IV) interacts directly with Co(II) at the oxide surface. All of the desorption data were preequilibrated for the same time period and collected after the same time so it is not known whether the retention of Co(II) is a result of slower desorption rates or thermodynamic irreversibility. To assess reproducibility, data were collected for a number of desorption experiments run under the same conditions. In all of the experiments, the single-sorbate desorption data coincided with single-sorbate sorption data, and there was an enhancement in cobalt retention at the lower surface coverages when Se(IV) was present.

## XAS Results

**Data Analysis.** Normalized background subtracted $k^3$ EXAFS spectra for Co(II) sorption samples are shown in conjunction with spectra for $Co(OH)_2$(s), aqueous Co(II) nitrate, and a Co−Al coprecipitate (Figure 2a). Aqueous Co(II) produces a sinusoidal type wave pattern descriptive of a cobalt−oxygen absorber-backscatter pair. For sorbed samples (numbers 2−5), the presence of cobalt backscattering results in an additional frequency superimposed on the sinusoidal wave as evidenced by shoulder "beat patterns" at approximately 5 $Å^{-1}$, 8 $Å^{-1}$, 9 $Å^{-1}$, and 11 $Å^{-1}$ which increase in intensity with increasing Co(II) coverage. Sorption samples with Se(IV) show a decrease in the size of these "beat patterns" with increasing Se(IV) surface coverage but no change in the presence of Se(VI). This suggests a decrease in second neighbor coordination or a change in structure for Se(IV) and unchanged coordination for Se(VI) samples.

**TABLE 2. Fit Parameters for 2 Week Co(II) Sorption Samples**

| | | | | Co−O | | | Co−Co | | | |
|---|---|---|---|---|---|---|---|---|---|---|
| sample | pH | $\Gamma_{Co}$ | $\Gamma_{Se}$ | *R* | *N* | $\Delta\sigma^2$ | *R* | *N* | $\Delta\sigma^2$ | $\Delta E_0$ |
| R1 | 7.45 | 1.60 | 0 | 2.08 | 5.85 | 0.003 | 3.09 | 2.16 | 0.003 | −5.56 |
| R2 | 7.55 | 1.56 | 1.65[a] | 2.08 | 6.06 | 0.003 | 3.09 | 2.36 | 0.003 | −6.16 |
| R3 | 7.58 | 1.21 | 1.65[b] | 2.08 | 5.50 | 0.004 | 3.12 | 0.91 | 0.005 | −5.95 |

[a] Se(VI). [b] Se(IV).

Cobalt RSFs for the sorption samples (uncorrected for phase shift) exhibit two main contributions similar to the cobalt hydroxide model (Figure 2b). The first peak is the oxygen backscattering contribution and the second is primarily cobalt backscattering. EXAFS spectra were fit using phase and amplitude functions generated by FEFF 7.0 (*32*) from $Co(OH)_2$(s). The best fit for cobalt XAFS spectra consisted of two components as shown in Table 1. The $Co(OH)_2$(s) standard was fit by fixing the first and second shell parameters to known crystallographic coordination numbers (*N*) and distances (*R*) while floating the Debye-Waller factor. The resulting fits conform to the data with a fit uncertainty of ± 20% for *N* and ± 0.02 Å for *R* based on evaluation of error of model compounds and fits in similar systems (*12*). The fit of the $Co(NO_3)_{2(aq)}$ sample was conducted in the same fashion as the unknowns and resulted in a single C−O shell with $N = 6$ and $R = 2.08$ Å as expected for hydrated cobalt. The Co−O distance in the sorption samples and precipitate were consistent with aqueous Co but significantly shorter than $Co(OH)_2$(s).

The first coordination shell was fit to six oxygen atoms at a distance of 2.08 Å in all samples. The second coordination shell corresponds to cobalt single scattering at a distance of 3.09 Å. Higher shell distances are evident from the RSF and are represented by third shell Co single scattering and multiple scattering paths. While these shells can be fit using experimental and theoretical models, the information does not conclusively add any new information relevant to this paper. Consequently, the following discussion focuses on single scattering paths of the first two shells.

Considering that coprecipitates with Al(III) are known to form under these conditions (*4*, *11*), aluminum should be present as a second shell neighbor to cobalt. Co−Al second shell fitting to extract structural parameters was conducted by constraining the Debye-Waller factor to be equal to the Co−Co value. Adding Al as a second component increased the Co coordination and Debye-Waller value with respect to the value obtained by fitting Co alone. In fact, in one case adding Al in the bisorbate sample fits increased the total coordination of the second shell relative to the single sorbate case, counter to the reduction shown in the RSF. Thus, not only were improvements to the overall fits not significant with the addition of Al, the results of the fits using Al may be unreliable. Two attributes make dependable fitting of Co and Al in the same shell difficult. First, backscattering from Al is much weaker than Co, resulting in Co dominating the overall contribution. The dominance of cobalt scattering means Co can be fit as a single component even if Al(III) is present. Second, amplitude cancellation occurs between the two components, resulting in poorly constrained coordination numbers (*11*). In turn, the strong correlation between *N* and $\sigma^2$ can result in fits which may be more influenced by the inherent uncertainty in the nonlinear least squares reduction than a physical structural significance. While the lack of a conclusive fit prevents direct evaluation of the role

**TABLE 3. Percent Reduction in Co−Co Coordination with Increasing Se(IV)-to-Co(II) Coverage Ratio**

| single solute sample | bisolute sample | $\Gamma_{Se}/\Gamma_{Co}$ | % N decrease in second shell |
|---|---|---|---|
| SS1 | BS1 | 0.81 | 10.2 |
| SS4 | BS5 | 1.46 | 62.5 |
| SS2 | BS3 | 1.62 | 41.8 |
| SS2 | BS4 | 2.00 | 100 |

of Al in the surface phase, the high degree of uncertainty does not preclude the presence of aluminum in the structure. Indeed, the consistency in atomic distances between the sorption samples, the Co−Al coprecipitate used in this study and coprecipitates previously reported (*11*, *21*−*23*), suggests the formation of a hydrotalcite-like precipitate.

Second shell Se fitting to extract structural parameters was also conducted in the bisorbate samples. Selenium phase functions are significantly different from cobalt, and the amplitude of selenium scattering should be sufficiently large as to avoid problems associated with aluminum. Thus, if selenium were present as a cobalt nearest neighbor, a significant change should be present in the spectra relative to the single sorbate case.

**Cobalt XAS Results.** Comparison of single sorbate samples SS2 and SS4 shows that second shell coordination increases with increasing cobalt surface coverage, consistent with previous findings of Co sorption to $\gamma$-$Al_2O_3$ by Chisholm-Brause (*10*). Second shell distances are significantly shorter than $Co(OH)_2$(s) and are consistent with distances of the Co−Al coprecipitate (sample PPT) and others previously reported (*11*, *22*). Based on these similarities, the dominant Co(II) surface phase in the single sorbate samples in this study is most likely a hydrotalcite-like precipitate with nitrate and possibly trace amounts of carbonate in the interlayer.

Comparison of second shell coordination values for single sorbate samples SS2 and SS4 with the bisorbate Se(VI) sample BS2 shows that second shell coordination is consistent with single sorbate Co(II) coprecipitation. EXAFS spectra of the Co(II)/Se(VI) sample shows no effect in coordination. Thus, the presence of Se(VI) had no effect on the structure of cobalt; consistent with macroscopic data showing no change in Co(II) sorption.

Comparison of single sorbate Co(II) samples with bisorbate samples of equal or higher Co surface coverage shows a decrease in Co−Co coordination in the presence of Se(IV) (samples SS1 and BS1, SS2, BS3, and BS4) (Figure 2b and Table 1). Furthermore, comparison of samples BS3 and BS4 shows that increasing the Se(IV) coverage at the same Co surface coverage results in the complete loss of second shell coordination at a Se(IV) coverage of 1.6 $\mu$mol/m$^2$. These results are consistent with the changes found in the EXAFS spectra and conclusively demonstrate that a structural change occurs to the Co(II) phase in the presence of Se(IV). Additional samples (Figure 3a,b and Table 2) that were reacted for 2 weeks compared with 2 days show the same reduction in cobalt second shell coordination, indicating that the new Co(II) phase is stable for at least 2 weeks. The same effect of Se(IV) on cobalt structure was found for the desorption bisorbate sample shown in Figure 3c,d (sample BS5). This sample showed a decrease in second shell coordination that was consistent with the reduction observed for the bisorbate Co(II)/Se(IV) sorption samples (e.g. sample BS3).

The amount of sorbed Se(IV) relative to Co(II) was varied among the samples. One way of evaluating the Se(IV) effect is to compare the samples based on the relative amounts of Se(IV) and Co(II) by using a ratio of Se(IV) to Co(II) surface coverage ($\Gamma_{Se}$:$\Gamma_{Co}$). Table 3 compares the coverage ratio with the percent change in the Co−Co coordination value between

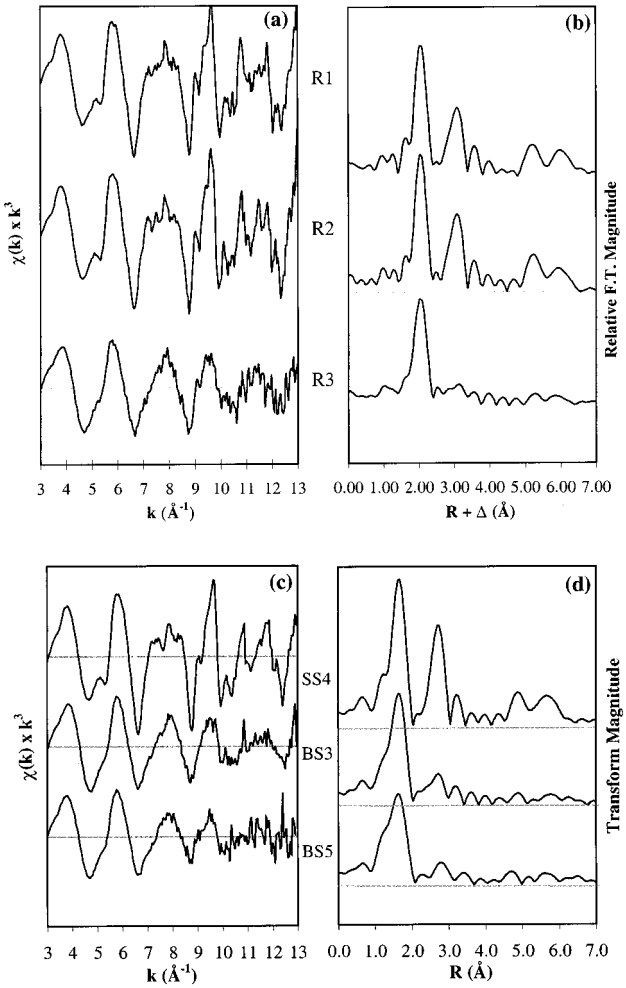


**FIGURE 3. Cobalt EXAFS results for samples reacted for 2 weeks and desorption sample. (a) Background subtracted, *k*-weighted cobalt EXAFS spectra for 2 week equilibration. (b) Radial structure functions of Fourier transformed EXAFS for 2 week equilibration. Fits are comparable to those shown in Figure 1c using parameters in Table 3. (c) Comparison of background subtracted, *k*-weighted cobalt EXAFS spectra for desorption sample (sample BS5), single-sorbate sorption sample (sample SS4), and bisorbate sorption sample (sample BS3). (d) Comparison of radial structure functions of Fourier transformed EXAFS for desorption sample, single-sorbate sorption sample, and bisorbate sorption sample. Fits are comparable to those shown in Figure 2c using parameters in Table 1.**

single and bisorbate samples of similar Co(II) surface coverage. Considering the high degree of uncertainty in coordination value (as much as 20%) and the fact that coverages are not exactly equal in all cases, the data demonstrate a remarkable trend. Increasing $\Gamma_{Se}$:$\Gamma_{Co}$ results in an increase in the fractional change to the second shell coordination number. The positive correlation between $\Gamma_{Se}$:$\Gamma_{Co}$ and the degree of structural change suggests that the presence of Se(IV) directly alters the Co(II) surface phase.

**Selenium XAS Results.** Background subtracted $k^3$ selenium EXAFS spectra are shown in Figure 4a for both Se(IV) and Se(VI) sorption samples. All spectra exhibit a single sinusoidal pattern consistent with the aqueous Se(IV) sample with the exception of a phase shift between Se(IV) and Se(VI). Single peaks corresponding to Se−O at a distance of 1.70 Å for Se(IV) and 1.65 Å for Se(VI) dominate selenium radial structure functions. First shell fit parameters (Table 4) show Se−O coordination of 3 ± 20% for Se(IV) and 4 ± 20% for Se(VI). Single sorbate Se(IV) sorption results are consistent with earlier studies by Papelis (*33*).

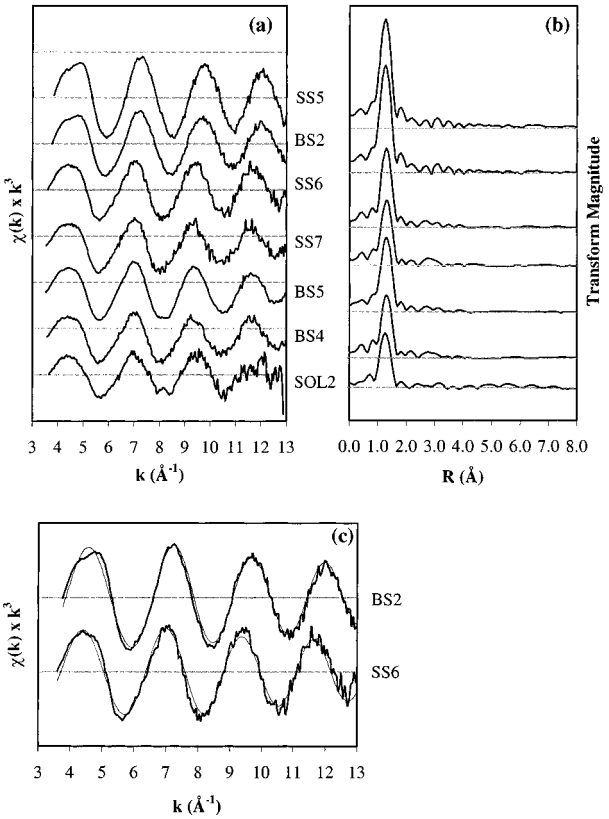


**FIGURE 4. Selenium EXAFS results. (a) Background subtracted $k^3$ selenium EXAFS spectra. See Table 1 for sample identification. (b) Fast Fourier transformed RSF uncorrected for phase shift. (c) Fit examples representative of the fit quality. Thick lines are the data and fine lines are the fits using parameters in Table 4.**

**TABLE 4. Fit Parameters for Selenium**

| | | surface coverage data | | | first shell, Se−O | | |
|---|---|---|---|---|---|---|---|
| sample | pH | $\Gamma_{Co}$ | $\Gamma_{SeO3}$ | $\Gamma_{SeO4}$ | *N* | *R* | $\sigma^2$ |
| MC2 | | $Na_2SeO_4$ 40 mg/1 g BN | | | 4.00 | 1.65 | 0.002 |
| BS2 | 7.32 | 1.0 | | 3.9 | 4.25 | 1.65 | 0.002 |
| SS5 | 7.64 | | | 1.2 | 4.99 | 1.65 | 0.002 |
| MC3 | | $Na_2SeO_3$ 40 mg/1 g BN | | | 3.00 | 1.70 | 0.002 |
| SOL2 | 9.60 | 0.1 M $Na_2SeO_3$ | | | | | |
| SS6 | 7.83 | | 0.8 | | 3.76 | 1.70 | 0.002 |
| SS7 | 7.84 | | 1.2 | | 3.51 | 1.71 | 0.003 |
| BS4 | 7.50 | 0.8 | 1.6 | | 3.01 | 1.71 | 0.002 |

## Discussion

While the spectroscopy data clearly demonstrate that Se(IV) has a direct impact on the structure of Co(II) sorbed species, the sorption mechanism responsible for the change is not clear. Several different types of sorption events that could explain the reduction in Co(II) sorption are discussed below. Three principle facts are used as a guide for identifying the mechanisms. First, the decrease in Co(II) sorption in the presence of Se(IV) occurs only at high cobalt surface coverages, indicating that the mechanism is related to coprecipitation. Second, bisorbate samples have equal to or greater Co(II) surface coverages than single sorbate samples, thus, indicating that a decrease in Co−Co coordination is not a result of lower Co(II) coverage in the bisorbate sample. Third, when making comparisons between the macroscopic data and EXAFS results it is important to distinguish between differences caused by pH versus surface coverage changes. The macroscopic sorption data show a decrease in sorption at the same pH for Co(II) in the presence of Se(IV), while the XAS data show a decrease in Co−Co coordination at the same coverage but different pH.

One possible mechanism for reduced Co(II) sorption is that sorbed Se(IV) blocks the formation of Co(II)-Al(III) coprecipitates by occupying neighboring surface sites (steric hindrance) or complexing available Al(III) (equilibrium controlled competition). Surface steric hindrance is unlikely based on a coprecipitate study by d'Espinose de la Caillerie et al. showing that coprecipitates can form away from the alumina surface (*22*). In their study, alumina was separated from the cobalt solution with a dialysis bag, and coprecipitates were found both inside and outside of the membrane. This indicates that Al(III) was transported away from the surface through the membrane because the molecular weight cut off would not allow coprecipitates to pass. Thus, coprecipitation can form away from the surface if Al is available in solution regardless of the amount of surface occupation by Se(IV).

Al(III) scavenging by Se(IV) could poison coprecipitate formation by limiting available Al(III). Se(IV) is known to form innersphere complexes with alumina and can form aluminum Se(IV) precipitates. Several aluminum Se(IV) hydrates have been prepared (*34*). A similar oxyanion, arsenate, was found to poison the growth of iron oxyhydroxide crystals through either a reduction in iron dissolution (*35*) or precipitation of iron arsenate (*36*). Benjamin and Bloom (*7*) suggested that the formation of iron arsenate as a new surface phase could be responsible for an increase in Cd(II) sorption in the presence of arsenate.

A greater proportion of mononuclear surface complexes in the bisorbate samples compared to the single sorbate coprecipitate samples could explain the shift in the Co(II) pH sorption edge to a higher pH. Greater deprotonation of surface sites would be required to achieve a surface coverage of mononuclear complexes equal to the single sorbate coprecipitate. This hypothesis supports the decrease in Co(II) sorption shown macroscopically during sorption because a decrease in precipitate formation reduces the removal of Co(II) from solution at a specific pH. However, the desorption bisorbate sample in which Se(IV) was introduced after the formation of a coprecipitate showed reduced Co−Co coordination similar to the bisorbate sorption samples, while coprecipitates should be present before the introduction of Se(IV). Furthermore, the desorption rate of Co(II) was reduced in the presence of Se(IV) compared to the single sorbate data. To achieve the reduction in Co−Co coordination while maintaining an equal surface coverage, cobalt surface speciation must be changing. The fact that the pH desorption edge falls to the left (lower pH) of the pH sorption edge is counter to the formation of more mononuclear complexes, even if the effect is kinetic. Instead, the effect of Se(IV) on Co(II) desorption suggests that Se(IV) is interacting directly with Co(II) at or near the surface.

The change in Co structure can also be explained by the formation of a different precipitate, which is either disordered or has lower Co−Co second shell coordination. The presence of a disordered structure could give rise to an apparent decrease in precipitate due to signal averaging. However, because the surface coverage of the bisorbate samples is equal to or greater than the single sorbate samples, a lower second shell amplitude in the bisorbate sample still indicates a change has occurred to the nature of the sorbed species. A bulk solution precipitate with Se(IV) is unlikely because all bisorbate solutions were undersaturated with respect to $CoSeO_3$ (*5*), and precipitates were not observed in blanks not containing $\gamma$-$Al_2O_3$. Furthermore, a solution precipitate would not necessarily limit other sorption mechanisms and would result in an increase in Co(II) sorption due to the excess of Se(IV) in the system. The fact that the surface induced coprecipitate phase is disrupted or changed and that

reduction of second shell cobalt is positively correlated with Se(IV) surface coverage is further evidence that the new phase is a surface phase rather than a solution phase. Potentially, Se(IV) is exchanging for nitrate in the hydrotalcite-like structure or forming a different mixed metal Se(IV) hydrate, resulting in a different atomic arrangement or reducing structural order.

Another interpretation of a disordered phase is a ternary Co(II)-Se(IV)-Al(III) surface complex. These complexes could be variable in orientation (i.e., double surface bonded and single surface bonded), reducing the ability to detect Co−Se contributions in the EXAFS. A higher relative amount of ternary complex compared to a Co(II)-Al(III) coprecipitate would reduce Co−Co coordination with increasing Se coverage. Furthermore, ternary complexes could act as weaker sorbing metals compared to free Co(II) ion, requiring greater surface deprotonation to achieve the same level of sorption as mononuclear adsorption complexes. However, unlike mononuclear complexes, ternary complexes are consistent with the desorption data. Bonding of the ternary complex through both the ligand and the metal is also consistent with a decrease in the rate of Co(II) desorption. Additionally, two pieces of evidence from the macroscopic data support the presence of ternary complexes. First, previous data show an increase in Se(IV) sorption in the bisorbate samples relative to single sorbate Se(IV) samples (*5*). The fact that Co(II) sorption is decreasing while Se(IV) sorption is increasing is consistent with the formation of a ternary Co−$SeO_3$−Al surface complex at the expense of the hydrotalcite-like phase. Second, the decrease in Co(II) sorption was greater at higher Co(II) surface loadings where the amount of coprecipitate should be greater based on the single sorbate case. Thus, when Se(IV) is present, the amount of Co(II) sorbed at a specific pH is controlled by the surface.

Unfortunately, the availability of formation constant data is limited for metal selenites. In a previous paper, we hypothesized that cobalt and aluminum selenite or hydrogen selenite complexes could occur based on formation constants of these metals with similar ligands (*5*). Determining formation constants and acquiring direct evidence of these species is key to evaluating the role of ternary complexes if they exist. However, even if these data were available, differentiating between ternary complexes and mixed metal Se(IV) hydrates or some other precipitate with direct spectroscopic evidence has proven to be a formidable task as evidenced by the results of this study. Nonetheless, these results illustrate that the cosorption of Co(II) in the presence of the oxyanion Se(IV) results in a new Co−Se−Al structure that can significantly change cobalt sorption behavior. Improved modeling of cation sorption in multisolute systems requires that such effects be better characterized both structurally and in terms of sorption behavior.

## Acknowledgments

The authors thank the staff at SSRL (supported by the Department of Energy and the National Institute of Health), especially Britt Hedman, for their assistance during our XAS beamtime. Chia-Chen Chen, Charlambis Papelis, and Samuel Traina have been invaluable members of our research team at SSRL. We also thank Samuel Traina and three anonymous reviewers for their helpful comments on this paper. This research was supported by the National Science Foundation, Grant Nos. BES-9625047 and BES-9896214.

## Literature Cited

(1) Hayes, K. F.; Katz, L. E. In *Physics and Chemistry of Mineral Surfaces*; Brady, P. V., Ed.; CRC Press: New York, 1996.
(2) Waite, T. D.; Davis, J. A.; Payne, T. E.; Waychunas, G. A.; Xu, N. *Geochim. Cosmochim. Acta* **1994**, *58(24)*, 5465−5478.
(3) Brown, G. E., Jr.; Parks, G. A.; Bargar, J. R.; Towle, S. N. In *Kinetics and Mechanisms of Reactions at the Mineral/Water Interface*; Sparks, D. L., Grundl, T. J., Eds.; ACS Symposium Series No. 715; 1999.
(4) Katz, L. E.; Boyle-Wight, E. J. In *Physical and Chemical Processes of Water & Solute Transport/Retention in Soils*; Selim, M., Sparks, D. L., Eds.; SSSA Symposium Series, in press.
(5) Boyle-Wight, E. J.; Katz, L. E.; Hayes, K. F. *Environ. Sci. Technol.* **2002**, *36*, 1212−1218.
(6) Tewari, P. H.; Lee, W. *J. Coll. Int. Sci.* **1975**, *52*, 77−88.
(7) Benjamin, M. M.; Bloom, N. S. In *Adsorption from Aqueous Solutions*; Tewari, P. H., Ed.; Plenum Press: New York, 1981.
(8) Schenck, C. V.; Dillard, J. G.; Murray, J. W. *J. Coll. Int. Sci.* **1983**, *95*(2), 398−409.
(9) Chisholm-Brause, C.; O'Day, P. A.; Brown, G. E., Jr.; Parks, G. A. *Nature* **1990**, *348*(6), 528−530.
(10) Chisholm-Brause, C. J. Ph.D. Dissertation, Stanford University, 1991.
(11) Towle, S. N.; Bargar, J. R.; Brown, G. E., Jr.; Parks, G. A. *J. Coll. Int. Sci.* **1997**, *187*, 62−82.
(12) O'Day, P. A.; Brown, G. E.; Parks, G. A. *J. Coll. Int. Sci.* **1994**, *165*, 269−289.
(13) O'Day, P. A.; Parks, G. A.; Brown, G. E. *Clays Clay Miner.* **1994**, *42*, 337−355.
(14) Papelis, C.; Hayes, K. F. *Colloids and Surfaces A.; Aspects* **1995**, *107*, 89−96.
(15) Chen, C. C.; Hayes, K. F. *Geochim. Cosmochim. Acta* **1999**, 63-(*19/20*), 3205−3215.
(16) Katz, L. E.; Hayes, K. F. *J. Coll. Int. Sci.* **1995**, *170*, 477−490.
(17) O'Day, P. A.; Brown, G. E., Jr.; Parks, G. A. Sixth Annual EXAFS Conference, 1990.
(18) Charlet, L.; Manceau, A. *Geochim. Cosmochim. Acta* **1994**, *58-(11)*, 2577−2582.
(19) Scheidegger, A. M.; Lamble, G. M.; Sparks, D. L. *J. Coll. Int. Sci.* **1997**, *186*, 118−128.
(20) Schiedegger, A. M.; Lamble, G. M.; Sparks, D. L. *Geochim. Cosmochim Acta* **1998**, *62*, 2233−2402.
(21) Thompson, H. A.; Parks, G. A.; Brown, G. E., Jr. *Clays Clay Miner.* **1999**, *47*, 425−438.
(22) d'Espinose de la Caillerie, J.-B.; Kermarec, M.; Clause, O. *J. Am. Chem. Soc.* **1996**, *117*, 11471−11481
(23) Thompson, H. A.; Parks, G. A.; Brown, G. E., Jr. *Geochim. Cosmochim. Acta* **1999**, *63*, 1767−1779
(24) Taylor, R. M. *Clay Miner.* **1984**, *19*, 591−603.
(25) Lytle, F. W.; Sandstrom, D. R.; Marques, E. C.; Wong, J.; Spiro, C. L.; Huffman, G. P.; Huggins, F. E. *Nucl. Instrum. Methods Phys. Res.* **1984**, *226*, 542−548.
(26) George, G. N.; Pickering, I. J. Stanford Synchrotron Radiation Laboratory: Menlo Park, CA, 1995.
(27) McMaster, W. H.; Nerr del Grande, N.; Mallett, J. H. Lawerence Radiation Laboratory, University of California, 1969.
(28) Teo, B.-K. In *EXAFS: Basic Principles and Data Analysis*; Springer-Verlag: New York, 1986.
(29) Brown, G. E., Jr.; Calas, G.; Waychunas, G. A.; Petiau, J. In *Spectroscopic Methods in Mineralogy and Geology*; Hawthorne, F. C., Ed.; Reviews in Mineralogy, No. 18, Mineralogical Society of America: Washington, DC, 1988; pp 431−512.
(30) Zabinsky S. I.; Rehr, J. J.; Ankudinov, A.; Albers, R. C.; Eller, M. J. *Phys. Rev. B* **1995**, *52(4)*, 2995−3009.
(31) Hayes, K. F., Ph.D. Dissertation, Stanford University, 1987.
(32) Rehr, J. J.; Mustre de Leon, J.; Zabinski, S. I.; Albers. R. C. J. *Am. Chem. Soc.* **1991**, *113*, 5135−5140.
(33) Papelis, C.; Brown, G. E., Jr.; Parks, G. A.; Leckie, J. O. *Langmuir* **1995,** *11*, 2041−2048.
(34) Morris, R. E.; Harrison, W. T. A.; Stucky, G. D.; Cheetham, A. K. *J. Solid State Chem.* **1991**, *94*, 227−235.
(35) Manceau, A. *Geochim. Cosmochim. Acta* **1995**, *59(17)*, 3647−3653.
(36) Waychunas, G. A.; Fuller, C. C.; Rea, B. A.; Davis, J. A. *Geochim. Cosmochim. Acta* **1996**, *60(10)*, 1765−1781.

*Received for review October 16, 2000. Revised manuscript received November 27, 2001. Accepted November 27, 2001.*

ES001774I